Tech Science Press

# A Spring-Layer Model for a Bi-Layered Plate-Strip with Initial Stress Through Imperfect Contact Interface

**Ahmet Daşdemir***

Department of Mathematics, Faculty of Arts and Sciences, Kastamonu University, Kastamonu, 37150, Turkey.

*Corresponding Author: Ahmet Daşdemir Email: ahmetdasdemir37@gmail.com.

**Abstract:** In this paper, we present our report on the forced vibration of a bi-layered plate-strip with initial stress resting on a rigid foundation induced by a time-harmonic force. The investigation is carried out according to the piecewise homogeneous body model with utilizing the three-dimensional linearized theory of elastic waves in initially stressed bodies (TLTEWISB). The materials of the body are chosen to be linearly elastic, homogeneous, and isotropic. The interface between the layers is assumed to be imperfect, and is simulated by the spring-layer model. A similar degree of imperfection on the interface is realized in the normal and tangential directions. The mathematical model for the problem under consideration is designed, and the system of the equations of motion is approximately solved by employing the finite element method (FEM). The numerical results explaining the influence of the parameter that characterizes the degree of corresponding imperfectness on the dynamic response of the plate-strip are presented. In particular, we demonstrate that the distributions of the normal stress become flat, as the normal-spring parameter increases.

**Keywords:** Incomplete contact; initial stress; spring-type imperfectness; dimensionless frequency; forced vibration

## 1 Introduction

Multilayered structures have received substantial attention because they are regularly encountered on a daily basis. The mechanical properties of the interface adhesive bonds play a key role in investigating the dynamic response of the body under consideration. Therefore, the imperfect contact conditions, which cause discontinuity in the displacement components, are of increasing importance. For instance, with regard to the assumption that stresses are continuous, but displacements are discontinuous across the interface, the widely used spring-type imperfectness of the interface is modeled, and it is observed that the jumps in displacement components are linearly proportional to the respective interface stress components. Different imperfect contact conditions are also encountered in the designation and production of the materials.

Many known factors determine the dynamical behavior of multilayered systems, including its geometry, the initial static stress, and the frequency of the dynamic force exerted. The influence of the initial stresses cannot be investigated with regard to classical linear theory of elasticity since it is non-linear. According to the preceding mechanical consideration, when the amplitudes of the deformations by a dynamic force of a system with initial deformation are gradually smaller than those of the static initial force, appropriate investigations can be conducted within the scope of the three-dimensional linearized theory of elastic waves in initially stressed bodies (TLTEWISB). This theory has been developed within the scope of elastodynamics, upon which more detailed information is available in the monographs by Guz [8,9] and Akbarov [5].

Due to technological demands and the need for economic use of materials, some interesting phenomena have been observed within the scope of TLTEWISB and its other version. Kepceler [11]

investigated the torsional wave propagation in the bi-material compounded cylinder with an imperfect interface in the absence of initial stresses. Hu et al. [13] considered the influence of identically applied initial pressures on the radial surfaces of a hollow cylinder composed of materials with a first power hypo-elastic constitutive model. Akbarov and Negin [4] studied the generalized Rayleigh wave dispersion in a system consisting of two axially pre-stressed covering layers and half-spaces with an imperfect interface. Kurt et al. [12] examined the extensional and flexural Lamb waves in the sandwiched plate consisting of a metal elastic middle-core layer imperfectly bonded to piezoelectric face layers. By analysis of this research, it is clear that the problems under consideration have complex structures. The forced vibration of a pre-stressed plate-strip with finite length resting on a rigid foundation under a time-harmonic force has been comprehensively studied employing the finite element method (FEM) by Akbarov et al. [2] (for plate-strip subjected to a perpendicular force) and [1] (for bi-layered plate-strip subjected to a perpendicular force), Eröz [7] for plate-strip subjected to an inclined force), Akbarov et al. [3] (for bi-layered plate-strip with shear-spring interface), and Daşdemir and Eröz [7] (for bi-layered plate-strip subjected to an inclined force).

The forced vibration of a pre-stressed bi-layered plate-strip subject to a time-harmonic external force resting on a rigid foundation, where shear- and normal-spring types of imperfect contact at the interface exist, has yet to be analyzed. The mathematical modeling used to present fundamental insights for characterizing the influence of the imperfection of the contact conditions between the layers is missing. To address this issue, mathematical modeling is designed within the scope of the piecewise homogeneous body model with the utilization of TLTEWISB, to investigate the imperfect contact conditions and the frequency response of the plate-strip with finite length. The numerical calculations are done by using the FEM. The problems studied by Akbarov et al. [1,2,3,6,7] are special cases of the current problem. Therefore, the findings presented in this paper can also be regarded as a development of the aforementioned papers, because imperfect contact conditions between the layers of the plate-strip for both the shear- and normal-spring types are satisfied.

## 2 Problem Statement

The problem is investigated in the plane-strain state within the scope of TLTEWISB by utilizing the piecewise homogeneous body model. The mathematical modeling is constructed according to the following theory.

Consider a bi-layered plate-strip with length $2a$ and thickness $h\ (=h_1+h_2)$, where $h_1$ and $h_2$ denote the thickness of the upper and lower layers, respectively. We assume that the materials of the layers are chosen to be linear, elastic, homogeneous, and isotropic. As shown in Fig. 1, the plate-strip is resting on a rigid foundation and is subjected to the action of a time-harmonic force. The Cartesian coordinates given by $x_i$ are associated with the initial state and coincide with the Lagrange coordinates $x_i'$ in the natural state.

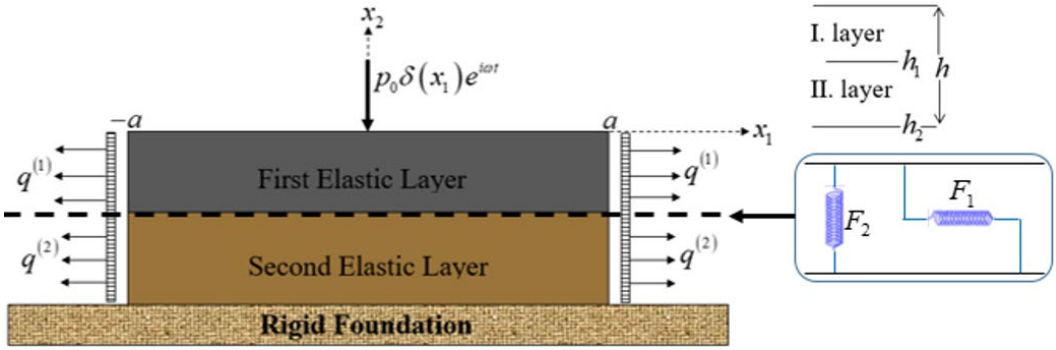


**Figure 1:** Geometry (left) and symbolic representation of the interface (right)

The length of the body along the direction of the $Ox_3$ axis is infinite. Since the force being applied to the body under consideration extends to infinity along this axis, the plane-stress-deformation state appears on the $Ox_1x_2$ plane. To represent the quantities related to the upper and lower layers, the upper indices "(1)" and "(2)" are respectively used, and the values for the initial state are denoted by the additional superscript 0. According to Fig. 1, the plate-strip lies in the domain $B = B_1 \cup B_2$, where

$$B_1 = \{(x_1, x_2) : -a \le x_1 \le a, -h_1 \le x_2 \le 0\},$$
$$B_2 = \{(x_1, x_2) : -a \le x_1 \le a, -h \le x_2 \le -h_1\}. \tag{1}$$

Each layer of plate-strip interacts with one another and with the rigid foundation after each of them is exposed by a homogeneous normal tension or compression force separately (only along the direction of the $Ox_1$ axis). Therefore, the uniaxial homogenous initial stress state occurs in the plate-strip. This initial stress is represented according to the linear theory of the elasticity, and written as

$$\sigma_{11}^{0,(m)} = q^{(m)} \text{ and } \sigma_{ij}^{0,(m)} = 0 \text{ for all } ij \ne 11, \tag{2}$$

where $q^{(m)}$ is a constant for each layer.

Guz [1,2] and Akbarov [5] express the general forms of the governing field equations under consideration as follows:

$$\sigma_{ij,j}^{(m)} + \left(\sigma_{kj}^{0,(m)} u_{i,k}^{(m)}\right)_{,j} = \rho^{(m)} \ddot{u}_i^{(m)}, \tag{3}$$

where $i; j; k; m = 1, 2$, $\rho^{(m)}$ is the mass density, $u_i^{(m)}$ is the displacement of the plate-strip in the $x_i$ direction, and $\sigma_{ij}^{(m)}$ are the stress tensor components. The dot over the quantities indicates time differentiation and the indices followed by the comma represent differentiation with respect to the relevant space-coordinate. The mechanical and geometrical relations for an isotropic elastic material between the stress and the displacement, respectively, can be written as

$$\sigma_{ij}^{(m)} = \lambda^{(m)} \varepsilon_{\ell\ell}^{(m)} \delta_{ij} + 2\mu^{(m)} \varepsilon_{ij}^{(m)} \text{ and } \varepsilon_{ij}^{(m)} = \frac{1}{2}\left(u_{i,j}^{(m)} + u_{j,i}^{(m)}\right), \tag{4}$$

where $\lambda^{(m)}$ and $\mu^{(m)}$ are the Lamé constants, and $\delta_{ij}$ is the Kronecker delta. Here and after this, the repeated subscript indices are summed over all possible index values.

Next, the boundary and contact conditions are considered. On the free surface of the plate-strip, the dynamic force condition

$$\sigma_{12}^{(1)}\Big|_{x_2=0} = 0, \ \sigma_{22}^{(1)}\Big|_{x_2=0} = -p_o \delta(x_1) e^{i\omega t} \tag{5}$$

is given, where $\delta(\cdot)$ is a Dirac delta function.

Because of the above initial stress that is applied to the edge of the plate-strip, the following boundary condition is satisfied.

$$\left(q^{(m)} u_{\mathrm{j},1}^{(m)} + \sigma_{1j}^{(m)}\right)\Big|_{x_1=\mp a} = 0. \tag{6}$$

The complete interaction at the interface plane between the considered body and rigid foundation are given by

$$u_j^{(2)}\Big|_{x_2=-h} = 0. \tag{7}$$

In addition to the preceding assumptions, it is believed that an imperfect contact interaction exists between the elastic layers. For the analysis presented herein, the imperfectness is described with reference

to a spring-layer model. This modeling is based on the assumption that stresses are continuous but the displacements are discontinuous across the interface. This means that there are jumps in the displacement components, namely these jumps are proportional to the tension components of the corresponding interface in terms of the spring-type interface parameters. Hence, it is believed that the displacement $\mathbf{u}^+$ and force $\mathbf{f}^+$ at one surface of an interface are proportional to the displacement $\mathbf{u}^-$ and force $\mathbf{f}^-$ at the other surface of the same interface, respectively. This approach can be written as

$$\left[\mathbf{f}\right]=\mathbf{G}\mathbf{u}^-+\mathbf{B}\mathbf{f}^- \text{ and } \left[\mathbf{u}\right]=\mathbf{A}\mathbf{u}^-+\mathbf{F}\mathbf{f}^-, \tag{8}$$

where $\mathbf{A}$, $\mathbf{B}$, $\mathbf{F}$, and $\mathbf{G}$ are square matrices, and $\left[.\right]$ indicates the jump in the corresponding quantities at the respective interface. In this paper, we consider the following case. Depending on the selection of the matrices $\mathbf{A}$, $\mathbf{B}$, $\mathbf{F}$, and $\mathbf{G}$ different incomplete contact situations can occur. Neglecting the matrix $\mathbf{G}$ and assuming that the matrices $\mathbf{A}$ and $\mathbf{B}$ are zero, we obtain the case investigated by Jones and Whittier [10], in matrix form:

$$\left[\mathbf{f}\right]=\mathbf{0} \text{ and } \left[\mathbf{u}\right]=\mathbf{F}\mathbf{f}^-, \tag{9}$$

where $\mathbf{F}$ is a constant diagonal matrix whose entries are identified in terms of the thickness and elastic constants of the investigated body. As a result, the imperfect contact conditions can be given mathematically as

$$\sigma_{i2}^{(1)}\Big|_{x_2=-h_1}=\sigma_{i2}^{(2)}\Big|_{x_2=-h_1},\ u_1^{(1)}-u_1^{(2)}=\frac{F_1h_1}{\mu^{(1)}}\sigma_{12}^{(m)}\Big|_{x_2=-h_1},\ u_2^{(1)}-u_2^{(2)}=\frac{F_2h_1}{\lambda^{(1)}+2\mu^{(1)}}\sigma_{22}^{(1)}\Big|_{x_2=-h_1} \tag{10}$$

where $F_1$ and $F_2$ are the shear- and normal-spring imperfect parameters, respectively and they are dimensionless varying over the ranges of $0\leqslant F_1, F_2\leqslant\infty$. The spring imperfectness creates three limiting cases. When $F_1=F_2=0$, the displacements are continuous at the interface. Therefore, the spring imperfectness approaches a welded interface. If $F_1\to\infty$ and $F_2\to\infty$, an unrestricted interaction occurs at the interface without mechanical contact. In the case wherein $F_1\to\infty$ and $F_2=0$, the displacements $u_2^{(m)}$ are continuous, but the displacements $u_1^{(m)}$ are discontinuous at the interface. Therefore, the spring imperfectness transforms into a slip interface.

This completes the presentation of the governing field equations and the corresponding boundary-contact conditions for the plate-strip shown in Fig. 1.

## 3 Solution Procedure

Since the problem under consideration has a complex structure and boundary-contact conditions, an analytical solution of the problem cannot be achieved. Therefore, the solution to this problem is approximated by using the FEM. Recall that the external force applied to the plate-strip is assumed to be time-harmonic with frequency $\omega$ as $p_o\delta(x_1)e^{i\omega t}$. Thus, all the corresponding dependent variables can be written in the form:

$$\left\{\sigma_{ij},u_i,\varepsilon_{ij}\right\}^{(m)}(x_1,x_2,t)=\left\{\overline{\sigma}_{ij},\overline{u}_i,\overline{\varepsilon}_{ij}\right\}^{(m)}(x_1,x_2)e^{i\omega t}, \tag{11}$$

where the superimposed bar represents the amplitude of the corresponding quantity. The dimensionless coordinate system is also introduced as

$$\hat{x}_1=\frac{x_1}{h},\ \hat{x}_2=\frac{x_2}{h}. \tag{12}$$

Substituting the expression in Eq. (11) into the previous equations and the conditions following the coordinate transformation in Eq. (12), the same equations and boundary-contact conditions are directly

found for the amplitude of the investigated quantities, changing the terms $\partial^2 u_j^{(m)}/\partial t^2$ and $p_o\delta(x_1)e^{i\omega t}$ with $-\omega^2 u_j^{(m)}$ and $p_o\delta(x_1)$, respectively.

To obtain FEM modeling of our last problem, the functional

$$J\left(\mathbf{u}^{(\mathbf{m})}\right)=\frac{1}{2}\sum_{m=1}^{3}\int_B\left[T_{ij}^{(m)}u_{j,i}^{(m)}-\left(\Omega^{(m)}\right)^2\left\{\left(u_1^{(m)}\right)^2+\left(u_2^{(m)}\right)^2\right\}\right]dB$$
$$+\frac{1}{2}\int_{-a/h}^{a/h}\left[F_1\frac{h_1}{h^2}\left(u_{1,2}^{(1)}+u_{2,1}^{(1)}\right)^2+F_2\frac{h_1}{h^2}\left(\frac{c_2^{(m)}}{c_1^{(m)}}u_{1,1}^{(1)}+\frac{c_1^{(m)}}{c_2^{(m)}}u_{2,2}^{(1)}\right)^2\right]\Bigg|_{x_2=-h_1/h}dx_1 \tag{13}$$
$$+\int_{-a/h}^{a/h}\frac{p_o\delta(x_1)}{\mu^{(1)}}u_2^{(1)}\Bigg|_{x_2=0}dx_1$$

is proposed, where

$$T_{ij}^{(m)}=\sigma_{ij}^{(m)}+\eta^{(m)}u_{j,n}, \tag{14}$$

$$c_1^{(m)}=\sqrt{\frac{\lambda^{(m)}+2\mu^{(m)}}{\rho^{(m)}}},\ c_2^{(m)}=\sqrt{\frac{\mu^{(m)}}{\rho^{(m)}}},\ \Omega^{(m)}=\frac{\omega h}{c_2^{(m)}},\ \eta^{(m)}=\frac{q^{(m)}}{\mu^{(m)}}, \tag{15}$$

In Eq. (15), $c_1^{(m)}$ is the speed of the dilatation waves, $c_2^{(m)}$ is the speed of the distortion wave, $\Omega^{(m)}$ denotes the dimensionless frequency of the plate-strip, and $\eta^{(m)}$ is the initial stress parameter of the $m$th layer.

Eq. (13) can be validated as follows: Considering the terms given in (14), using the Gauss theorem and computing the statement "$\delta J\left(\mathbf{u}^{(\mathbf{m})}\right)=0$", which is the first variation of the function in (13); the equations of motion in (3) and the relevant boundary-contact conditions in (5-7) and (10) that construct the problem are found. Thus, the desired proof is completed.

To carry out the FEM modeling of the problem under consideration, the virtual work principle and the standard Rayleigh-Ritz method are adopted, as stated by Zienkiewicz and Taylor [15]. With this approach, the domain B is divided into a finite element of sub-domains whose structures are nine-node smooth rectangular elements. The number of these finite elements is determined by the desired numerical convergence requirement. After certain mathematical adjustments, a system of algebraic equations

$$\left(\mathbf{K}\text{-}\omega^2\mathbf{M}\right)\tilde{\mathbf{u}}=\mathbf{F} \tag{16}$$

is obtained. In Eq. (16), $\mathbf{K}$ is the stiffness matrix, $\mathbf{M}$ is the mass matrix, $\tilde{\mathbf{u}}$ is the unknown nodal displacement vector, and $\mathbf{F}$ is the force vector. The explicit forms of the matrices and vectors are not provided herein; the explicit forms are derived from Eq. (13) using the proposed procedure. Therefore, the FEM modeling of the problem under consideration is completed.

## 4 Results and Discussions

The key objective of this study is to investigate the influence of the spring-type imperfect parameters (in both the normal and tangential directions) on the dynamic behavior of the plate-strip under consideration. Before giving the analysis of the numerical results, some explanations are required. The following notations are introduced: $e=E^{(1)}/E^{(2)}$, where $E^{(m)}$ is the Young modulus of $m$th layer. It can be derived that the distributions of stress components at the interface plane between the layers and on the bottom surface of the plate-strip have the same oscillating character in the qualitative sense. Since the force applied to the body under consideration is perpendicular to its free surface, the graphs are

symmetrical about $x_1/h$. All the following calculations are made on the surface for those parts of the diagrams where $x_1/h \geq 0$, and on the bottom after this. This does not impair the validity of the numerical results under consideration. In the analysis, the situation where Aluminum (Al) with properties $\nu^{(Al)} = 0.35$ and $\rho^{(Al)} = 2.7 \times 10^3$ at the upper layer and Steel (St) with properties $\nu^{(St)} = 0.29$ and $\rho^{(St)} = 7.86 \times 10^3$ at the lower layer is considered under $h/2a = 0.2$, $h_1 = h_2$, $\Omega = \Omega^{(1)} = \Omega^{(2)} = 0$, $\eta = \eta^{(1)} = \eta^{(2)} = 0$ and $\mathrm{F} = F_1 = F_2$ unless otherwise indicated.

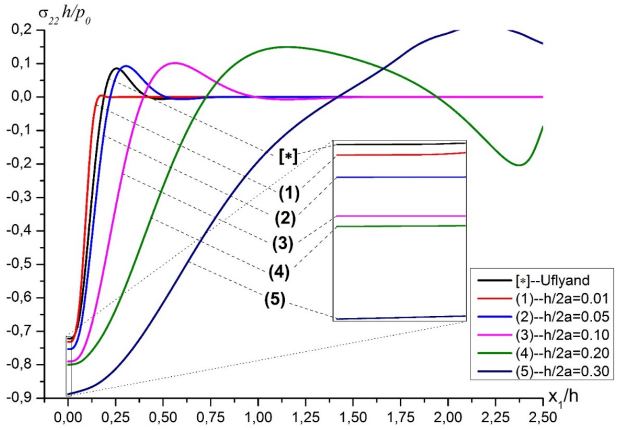


**Figure 2:** The variation of $\sigma_{22}h/p_0$ *vs.* the line $x_1/h$ for various thickness ratios under $e = 1$, $\nu^{(1)} = \nu^{(2)} = 0.33$ and $\mathrm{F} = 0$

To prove the validity of the programs used, the case where $e = 1$, $\nu^{(1)} = \nu^{(2)} = 0.33$ and $\mathrm{F} = 0$ is examined. Uflyand [14] considered the case for the plate with infinite length, and the problem was resolved. It can be demonstrated that the geometry of the plate-strip under consideration begins to resemble the one investigated by Uflyand as $h/2a \to 0$. In this situation, the numerical results given by the current FEM algorithm must converge to the corresponding ones from the one, which is the asterisked graph in Fig. 2, given by Uflyand [14]. This speculation is proven by the graphs in Fig. 2, and hence the validity and trustworthiness of the algorithm and programs.

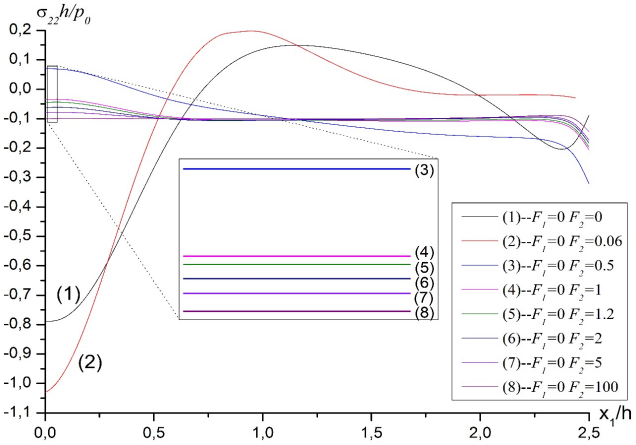


**Figure 3:** The distribution of $\sigma_{22}h/p_0$ *vs.* the line $x_1/h$ for normal spring-type parameter $F_2$ under $e = 1$, $\nu^{(1)} = \nu^{(2)} = 0.33$ and $F_1 = 0$

Akbarov et al. [3] investigated the situation where only shear-spring-type imperfect contact exists between the layers. To compare the influence of the normal spring-type imperfectness on the distribution of $\sigma_{22}h/p_0$ with that of the shear-spring-type imperfectness, Fig. 3 is provided for the case where $F_1=0$ and $F_2\geq 0$ under $e=1$ and $\nu^{(1)}=\nu^{(2)}=0.33$, where only the normal spring-type imperfect contact exists between the layers. As can be seen from the graphs, an increase in the value of the parameter $F_2$ ensures the identical distribution of normal stress $\sigma_{22}h/p_0$ with respect to the line $x_1/h$. In particular, the difference between the consecutive value of the stress $\sigma_{22}h/p_0$ at the point $(0,-1)$ damps quickly. In addition, it follows from the graphs in Fig. 3 that the numerical values of $\sigma_{22}h/p_0$ converge to a particular asymptotic value with the parameter $F_2$. This is explained by the case where $F_1=0$ and $F_2\to\infty$, where the displacements $u_1^{(m)}$ are continuous but the displacements $u_2^{(m)}$ are discontinuous at the interface, such that the upper layer is pushed to the lower layer with the assistance of current loading, such as a punch loading.

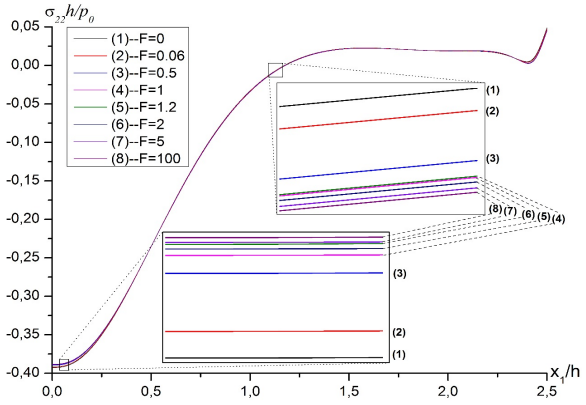


**Figure 4:** The distribution of $\sigma_{22}h/p_0$ *vs.* the line $x_1/h$ for a normal- and shear- spring-type parameter F under a pair of Al + St

In the case wherein both normal- and shear-spring-type imperfect contacts exist between the layers, the distribution of the stress $\sigma_{22}h/p_0$ with respect to the line $x_1/h$ for various values of the parameter F is given in Fig. 4 under the same assumptions defined in Fig. 3. The graphs show that the absolute values of the normal stress $\sigma_{22}h/p_0$ decrease with an increase in parameter F. However, comparison of Fig. 3 and Fig. 4 indicates that the distributions of the stress $\sigma_{22}h/p_0$ in Fig. 4 are relatively gradual processes. In addition, the values of the stress $\sigma_{22}h/p_0$ are independent of the selected parameter F for certain values of $x_1/h$. The numerical results given in Fig. 3 show that, in the case where $\mathrm{F}\to\infty$, the absolute values of $\sigma_{22}h/p_0$ converge to a certain asymptotic one with the parameter F, and that this asymptote relates to the case of full slipping at the interface.

Fig. 5 displays the dependence between the stress $\sigma_{22}h/p_0$ and $\Omega$ for various values of imperfect parameter F. In addition, various values of the ratio $h/2a$ are considered with the construction of these graphs. It can be seen from these graphs that there exist certain locations where $\sigma_{22}h/p_0$ reaches an extreme for particular values of $\Omega$. These values are known as the resonance values denoted by $\Omega^*$. The numerical results indicate that the values of $\Omega^*$ decrease with an increase in the ratio $h/2a$. The conclusion is that the effect of the parameter F on the values of $\Omega^*$ is notable not only quantitatively, but also qualitatively. The parameter F has a great influence on the resonance mode of $\sigma_{22}h/p_0$. An increase in the value of the ratio $h/2a$ causes a reduction in the influence of the imperfect parameter F

on the distribution of $\sigma_{22}h/p_0$. The normal stress $\sigma_{22}h/p_0$ has the parametric resonance at certain locations for certain values of the parameter F (denoted by $F^*$). These values of $F^*$ change with the ratio $h/2a$. An increase in the values of $h/2a$ causes a decrease in the numbers of the local maxima and minima of the normal stress $\sigma_{22}h/p_0$ versus the dimensionless frequency $\Omega$.

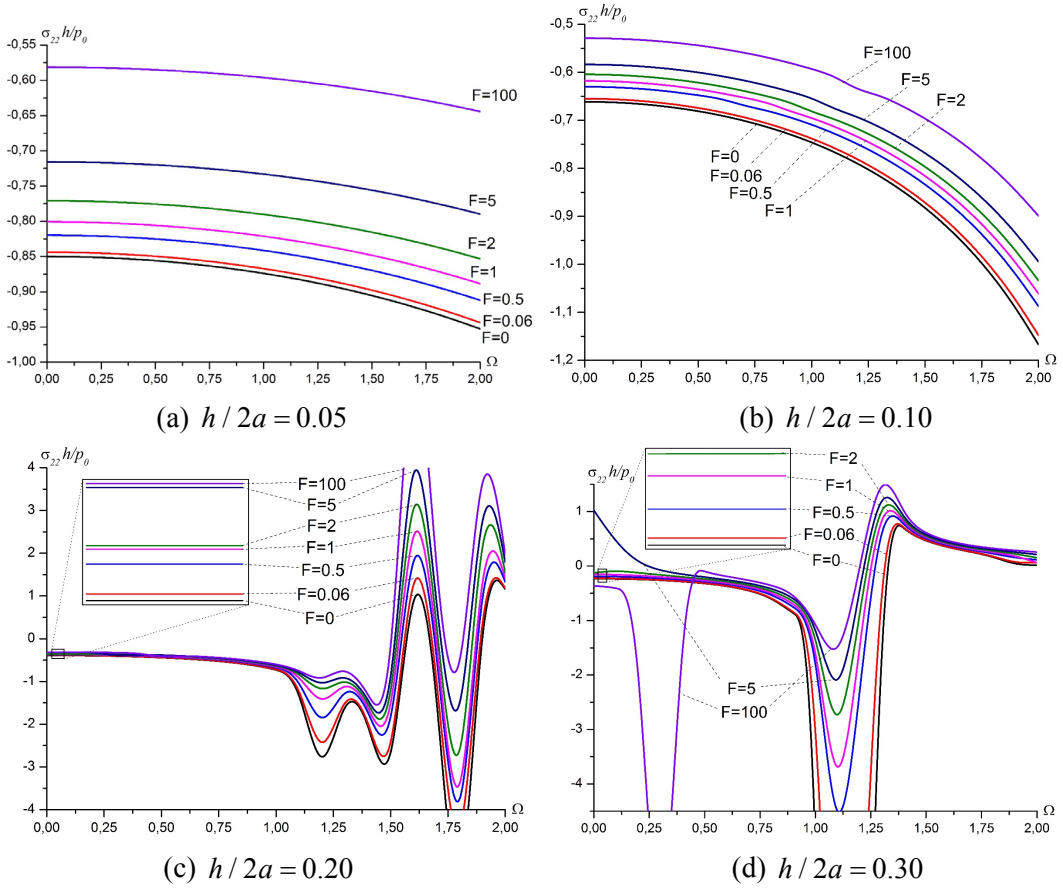


**Figure 5:** The distribution of $\sigma_{22}h/p_0$ *vs.* the dimensionless frequency $\Omega$ for various normal + shear spring type parameter F under a pair of Al + St: (a) h/2a = 0.05, (b) h/2a = 0.10, (c) h/2a = 0.20, (d) h/2a = 0.30

These discussions are made without reference to the initial stress in each layer. Therefore, in Fig. 6, the influence of the initial stress parameter $\eta$ on the dependence between $\sigma_{22}h/p_0$ and $\Omega$ is analyzed. Correspondingly, numerical results are given for various values of the imperfect parameter F. A comparison of the graphs in Fig. 6 reveals that the initial tension of the layers causes a decrease; however, the initial compression causes an increase in the absolute values of the normal stress $\sigma_{22}h/p_0$. The influence of the initial stresses on the frequency response of the stress $\sigma_{22}h/p_0$ in the case wherein the spring-type imperfection exists between the layers is more considerable compared with when the layers are in complete contact. The imperfect parameter F changes the character of the influence of the initial stress of the layers on the frequency response of the plate-strip. It can be demonstrated that an increase in the values of initial tension parameter leads to the decrease in its resonance by contrast with the influence of the compression parameter. In addition, the number of the parametric resonance of $\sigma_{22}h/p_0$ arisen in certain values of the initial stress parameter $\eta$ decreases as the imperfect parameter F increases.

## 5 Conclusions

In this study, the forced vibration induced by a time-harmonic external force of a pre-stressed plate-strip with two imperfectly bonded elastic layers, which rest on a rigid foundation, has been investigated. This has been done based on the fundamental principles of the TLTEWISB in the case where both shear- and normal-spring-type imperfections exist between the layers. The mathematical problem is created for consideration and numerically solved using FEM. Numerical results have demonstrated the influence of the change in imperfectness on the frequency response of the normal stress, acting on the interface planes between the plate-strip and rigid foundation. Numerical investigations have shown the following:

- the variation of the stress $\sigma_{22}h/p_0$ with respect to the line $x_1/h$ possesses an identical distribution when increasing the normal spring parameter $F_2$;
- an increase in the values of the parameter F causes the resonance mode of the normal stress $\sigma_{22}h/p_0$ to vanish;
- the imperfect interaction between the layers affects the character of the influence of the initial stresses on the frequency response of plate-strip;
- and the numbers of the local maxima and minima of the stress $\sigma_{22}h/p_0$ versus the dimensionless frequency $\Omega$ decrease with increasing the ratio $h/2a$.

The numerical results listed above have been presented under two different cases (for example a pair of Al + St), but note that they also have a general validity in a qualitative sense.

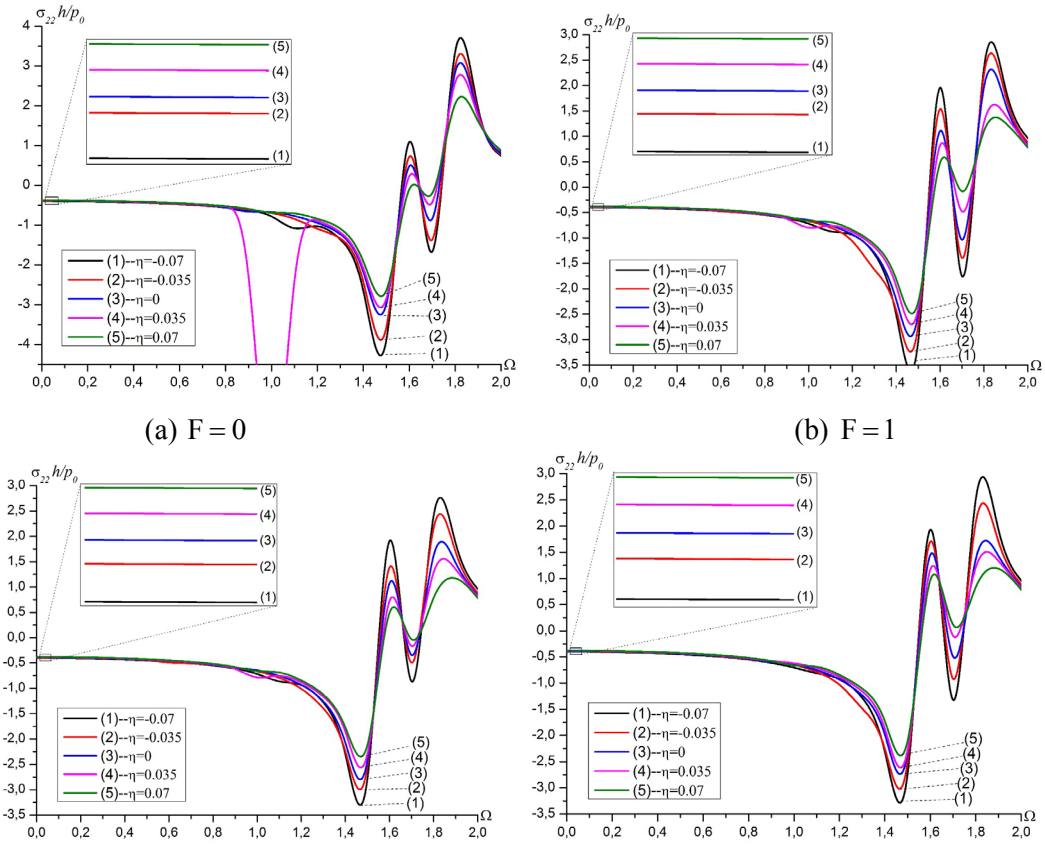


(a) F = 0 (b) F = 1

(c) F = 2 (d) F = 5

**Figure 6:** The distribution of $\sigma_{22}h/p_0$ *vs.* the dimensionless frequency $\Omega$ various initial stress parameter $\eta$ under a pair of Al + St: (a) F = 0, (b) F = 1, (c) F = 2, (d) F = 5

**Acknowledgement:** The author is a member of the research project supported by Research Fund of Kastamonu University under project number KÜBAP-01/2016-4. The author also wishes to thank anonymous referees for their suggestions, which led to substantial improvement of this paper.

## References

1. Akbarov, S. D., Yildiz, A., Eröz, M. (2011). FEM modelling of the time-harmonic dynamical stress field problem for a pre-stressed plate-strip resting on a rigid foundation. *Applied Mathematical Modelling, 35(2),* 952-964.
2. Akbarov, S. D., Yildiz, A., Eröz, M. (2011). Forced vibration of the pre-stressed bi-layered plate-strip with finite length resting on a rigid foundation. *Applied Mathematical Modelling, 35(1),* 250-256.
3. Akbarov, S. D., Hazar, E., Eröz, M. (2013). Forced vibration of the pre-stressed and imperfectly bonded bi-layered plate strip resting on a rigid foundation. *Computers, Materials & Continua, 36(1),* 23-48.
4. Akbarov, S. D., Negin, M. (2017). Near-surface waves in a system consisting of a covering layer and a half-space with imperfect interface under two-axial initial stresses. *Journal of Vibration and Control, 23(1),* 1-14.
5. Akbarov, S. D. (2015). *Dynamics of pre-strained bi-material elastic systems: linearized three-dimensional approach*. Springer.
6. Daşdemir, A., Eröz, M. (2015). Mathematical modeling of dynamical stress field problem for a pre-stressed bi-layered plate-strip. *Bulletin of the Malaysian Mathematical Sciences Society, 38(2),* 733-760.
7. Eröz, M. (2012). The stress field problem for a pre-stressed plate-strip with finite length under the action of arbitrary time-harmonic forces. *Applied Mathematical Modelling, 36(11),* 5283-5292.
8. Guz, A. N. (1986a). *Elastic waves in a body initial stresses, I. general theory*. Naukova Dumka.
9. Guz, A. N (1986b). *Elastic waves in a body initial stresses, II. propagation laws*. Naukova Dumka.
10. Jones, J. P., Whittier, J. S. (1967). Waves at a flexibly bonded interface. *Journal of Applied Mechanics, 34(4),* 905-909.
11. Kepceler, T. (2010). Torsional wave dispersion relations in a pre-stressed bi-material compounded cylinder with an imperfect interface. *Applied Mathematical Modelling, 34(12),* 4058-4073.
12. Kurt, I., Akbarov, S. D., Sezer, S. (2016). Lamb wave dispersion in a PZT/metal/PZT sandwich plate with imperfect interface. *Waves in Random and Complex Media, 26(3),* 301-327.
13. Hu, W. T., Xia, T. D., Chen, W. J. (2014). Influence of lateral initial pressure on axisymmetric wave propagation in hollow cylinder based on first power hypo-elastic model. *Journal of Central South University, 21(2),* 753-760.
14. Uflyand, Y. S. (1967). *Integral transformations in the theory of elasticity*. Nauka.
15. Zienkiewicz, O. C., Taylor, R. L. (1989): *The finite element method, basic formulation and linear problems*. McGraw-Hill.